Phys. Status Solidi RRL **10**, No. 12, 861–865 (2016) / **DOI** 10.1002/pssr.201600272

Impact of the firing temperature profile on light induced degradation of multicrystalline silicon

Rebekka Eberle[*,1], Wolfram Kwapil[,1,2], Florian Schindler[1,2], Martin C. Schubert[1], and Stefan W. Glunz[1,3]**

[1] Fraunhofer Institute for Solar Energy Systems ISE, Heidenhofstraße 2, 79110 Freiburg, Germany
[2] Freiburger Materialforschungszentrum (FMF), Albert-Ludwigs-Universität Freiburg, Stefan-Meier-Straße 21, 79104 Freiburg, Germany
[3] Technische Fakultät, Albert-Ludwigs-Universität Freiburg, Georges-Köhler-Allee 101, 79110 Freiburg, Germany

Received 11 August 2016, revised 21 October 2016, accepted 21 October 2016
Published online 26 October 2016

Keywords multicrystalline silicon, light-induced degradation, temperature profile, heat ramp

[*] Corresponding author: e-mail rebekka.eberle@ise.fraunhofer.de, Phone: +00 497 614 588 5588, Fax: +00 497 614 588 9250
[**] e-mail wolfram.kwapil@ise.fraunhofer.de, Phone: +00 497 614 588 5461, Fax: +00 497 614 588 9250

Light- and elevated temperature-induced degradation in multicrystalline silicon can reduce the efficiency of solar cells significantly. In this work, the influence of the firing process and its temperature profile on the degradation behaviour of neighbouring mc-Si wafers is analysed. Five profiles with measured high peak temperatures ≥800 °C and varying heating and cooling ramps are examined. With spatially resolved and lifetime calibrated photoluminescence images, normalized defect concentrations N_t^* are calculated to determine the degradation intensity. Wafers that underwent a fast firing process typical for industrial solar cell production show a significantly stronger degradation than samples that were subjected to the same peak temperature but with slower heating and cooling rates. A spatially resolved analysis of the carrier lifetime in the whole wafer shows that the degradation begins in low lifetime areas around dislocation clusters, spreading into good grains after several hours. By the use of optimized ramp-up and/or ramp-down rates during the firing even at very high peak temperatures, light and elevated temperature induced degradation can be suppressed.

1 Introduction Recent advances in the industrial PERC (passivated emitter and rear contact) cell technology in combination with improvements in crystallization techniques for high-performance multicrystalline silicon (HP mc-Si) have resulted in an impressive new mc-Si world record efficiency of 21.25% [1]. However, in 2012 a new degradation mechanism was observed at conditions relevant for module operation resulting in significant efficiency losses in such cells [2], which cannot be attributed to the boron-oxygen defect or iron-boron pairs [2–6]. Due to its dependence on temperature during illumination, this new defect was called light- and elevated temperature-induced degradation (LeTID) [7–9], although it can also be induced by current [7]. After the degradation process the multicrystalline material also shows a regeneration behaviour which can be accelerated by higher temperatures and light exposure [7–9]. The degradation influences the cell efficiency by reducing short-circuit current, open-circuit voltage and fill factor [7, 10]. Further research has shown that LeTID is also dependent on the firing temperature during cell production, the degradation being more pronounced at higher peak firing temperatures [11, 12]. Moreover, an additional second firing step at reduced temperatures can lead to a suppression of LeTID [9]. Our first experiments with boron-doped and phosphorus-gettered lifetime samples fired in a rapid thermal processing (RTP)-oven at relatively high peak temperatures (700–850 °C measured) showed a very small degradation in the range of $\Delta\tau = 10\%_{rel}$ at $\Delta n = 10^{15}$ cm^{-3}. This value seemed to be very low compared to the values reported in literature, those experiments having been conducted in fast firing ovens (FFO). However, a direct comparison was impossible due to other strong influences as peak firing temperature, material quality and gettering efficiency. Therefore, we

carried out an experiment to analyse the influence of the firing process itself and the temperature profile in particular on LeTID, keeping all other influences constant.

2 Experimental

2.1 Sample preparation Commercial high performance multicrystalline silicon wafers (cut to format 125 mm × 62.5 mm before processing) with a base resistivity of 1.0 Ω cm (boron doping) were taken from neighbouring positions in the ingot. All samples at first underwent the same process sequence: After a saw damage etch and HNF/SC1 cleaning, they were $POCl_3$-diffused at 847 °C for one hour, which resulted in a sheet resistance of ~50 Ω/sq, in order to achieve an efficient impurity gettering. The phosphorus silicate glass and the emitter were etched back. The wafers were covered with an Al_2O_3 layer (10 nm) and capped with a PECVD anti-reflective coating made of silicon nitride (100 nm). Finally, five different firing profiles, which were also used for the activation of the surface passivation, were applied. Since the heating and cooling rates in the RTP furnace are limited to <50 K/s whereas the FFO only allows for faster rates >80 K/s, the wafers were fired in two different furnaces. Having calibrated the peak temperatures and profiles in both furnaces on identically processed sister wafers – ensuring identical heating conditions – by using type K thermocouples, the target peak temperature for most of the samples was set to 800 °C, thus the temperature ramps being the only parameter variation. In order to check the significance of the firing temperature on LeTID in the RTP furnace, one temperature profile with a peak at 850 °C was added to the experiment. The measured temperature profiles on the sister samples are shown in Fig. 1. The standard FFO process (black solid line, 3 samples) shows a very fast heating and cooling of the wafers (120 and 70–80 K/s, respectively) as the samples leave the furnace right after having reached the maximum temperature. For all firing processes in the RTP furnace (1 sample per process) the temperature profile during the heating-up is identical (~50 K/s), being lower compared to the FFO process. Since it is known from literature that the cooling ramps of high temperature steps can have a significant impact on the final defect concentration through internal gettering [13], we intended to manipulate the defect responsible for LeTID by additional variations of the cooling ramps of the four RTP processes. The first variations ("RTP standard 800 °C", green dash-dotted line and "RTP standard 850 °C", orange dash-dotted line) imitate the FFO process as they feature fast cooling ramps but with different peak temperatures. In the RTP process labelled "with plateau" (red dashed line), after a slow cool at 30 K/s, a temperature plateau where the temperature was held stable at around 550 °C for 10 seconds was applied before the cooling process was continued. For the last variation ("RTP slow ramp"), a very slow but continuous cooling ramp of 10 K/s was used (blue dotted line). Although the peak temperatures have been set to the same value for four of the firing processes, slight deviations of the actual peak sample temperature of ±10 K are obvious in Fig. 1. However, the significant trends of our results cannot be explained by these relatively small differences.

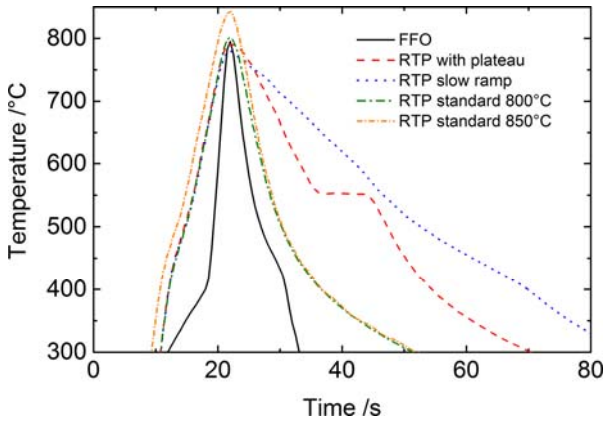

Figure 1 Temperature profiles of the firing processes (see text for details).

2.2 Measurements Carrier lifetime of the samples was characterized by injection-dependent photoluminescence (PL) imaging, covering a range of $\Delta n = 10^{11}$–10^{16} cm^{-3}, before and during the degradation process. PL imaging was performed with a 790 nm laser and a silicon CCD camera featuring a stack of long pass filters to suppress detection of laser light in combination with a 1000 nm short pass filter to reduce optical blurring. The PL images were calibrated to effective lifetimes τ_{eff} using harmonically modulated PL [14]. In order to begin the experiment in a defined state of the BO-complex, the samples were subjected to illumination at an intensity of ~0.15 suns (48 hours, room temperature) prior to the actual light- and temperature-induced degradation [15]. Since a lifetime regeneration due to the BO defect can occur during the LeTID treatment which cannot easily be separated from the specific mc-Si defect, the normalized BO defect concentration of the samples measured prior to LeTID is represented as error bars in Fig. 2. To ensure that the wafers were always measured in the same state of the Fe_i-/FeB metastability, the FeB-pairs were split by illumination before and in-between the measurement steps [16]. For the LeTID process, the samples were illuminated with halogen lamps at an intensity of ~1 sun and at a temperature of 75 °C. The defect responsible for the degradation was analysed by the effective normalized defect concentration N_t^* which is calculated with the initial and degraded lifetime at the same injection level Δn [17]:

$$N_t^*(\Delta n) = \frac{1}{\tau_{deg}(\Delta n)} - \frac{1}{\tau_{ini}(\Delta n)}. \quad (1)$$

All presented results were calculated with interpolated lifetimes at $\Delta n = 8 \times 10^{13}$ cm^{-3}. This value was covered by the measurements on all samples at every state of degradation and since the degradation was observed at all injection levels, this choice has no influence on the overall conclusions.

3 Results The normalized defect concentration N_t^* for all fired samples over degradation time is shown in Fig. 2. The results were calculated from lifetimes which were averaged over the whole wafer area. The FFO sample shows the highest values for N_t^* and therefore exhibits the strongest degradation of all samples. The wafers fired in all RTP processes show a significantly smaller degradation, the normalized defect concentrations staying more than an order of magnitude below the fast-fired samples. This is even true for the RTP-sample fired at 850 °C. We observe no significant difference in the defect evolution of the RTP samples even when applying a slower ramp or a medium-temperature plateau. As the peak temperature for the different firing processes was always approximately at the same level with one RTP peak temperature even significantly exceeding the FFO value, we can exclude the peak temperature being the reason for the large differences. This observation is in line with all our previous experiments on LeTID employing the RTP furnace on various mc-Si materials and using peak temperatures between 700 °C and 850 °C.

Images of the lifetime evolution for an FFO- and for an exemplary RTP sample ("with plateau") are shown in Figs. 3 and 4, respectively.

After an initial slow degradation, the FFO samples exhibit a drastic change in the lifetime evolution after more than 10 hours of illumination. Starting from the dislocation clusters, low lifetime areas "spread" throughout the whole wafer. Good grains close to highly dislocated areas seem to disappear and lifetimes drop from more than 300 µs to even below 10 µs at an illumination intensity corresponding to 1 sun. Only at the sample edges, hardly any degradation is observed. After more than 100 hours of the experiment, regeneration sets in and low lifetime areas start to recover again. Although also low lifetime areas in the wafer centre show already some improvement, the carrier lifetime recovers most strongly close to the edge areas where degradation proceeded most recently. The point in time when regeneration begins seems to be approximately the same for all wafer areas independent of the local defect concentration. Furthermore, as can be seen in Fig. 3(c) and (d), in the degraded state the carrier lifetime at grain boundaries is higher than in grains in the sample centre. Consequently, the defect concentration N_t^* is lower at grain boundaries which is consistent with observations from [17]. In contrast to the FFO samples, the degradation in the RTP samples (see Fig. 4) is much less pronounced. The lifetime decreases almost homogeneously. Interestingly, regeneration sets in at approximately the same time as for the FFO wafers, substantiating the observation that the starting time of regeneration is independent of the defect concentration.

To exclude the possibility that the FFO process – in contrast to the RTP processes – may (i) have harmed the surface passivation stack or (ii) have introduced deleterious impurities due to the immediate contact between the furnace belt and the samples, a float zone silicon reference sample (p-type, 1.0 Ωcm, 4 inch, 200 µm) featuring identical sample preparation was fired in the FFO with the same parameters. During the LeTID process, the sample shows no

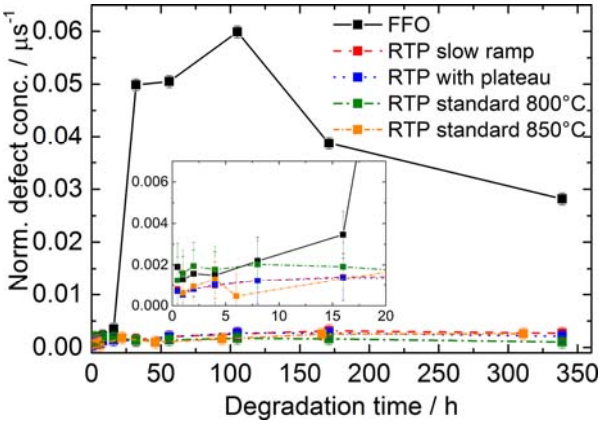

Figure 2 Normalized defect concentration N_t^* for all samples over degradation time, averaged over the whole wafer area. The inset shows a zoom-in of the first 20 hours of degradation.

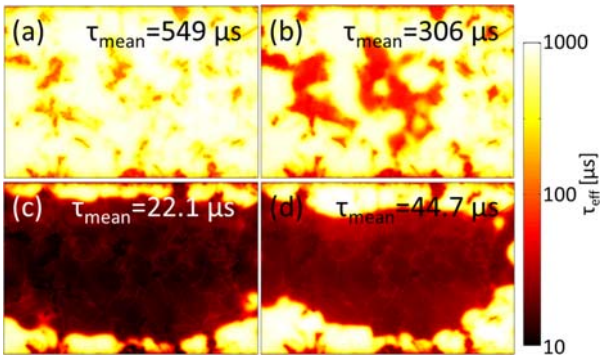

Figure 3 Lifetime calibrated PL images at an illumination intensity of 1 sun of an FFO sample (125 mm × 62.5 mm) at different time steps during degradation at ~1 sun and 75 °C. (a) Initial state, (b) after 16 hours of illumination, (c) after 105 hours, (d) after 339 hours. The logarithmic scaling, which is used to visualize the higher lifetime at grain boundaries in the degraded state, applies to all images. For a linear scaling see Supporting Information.

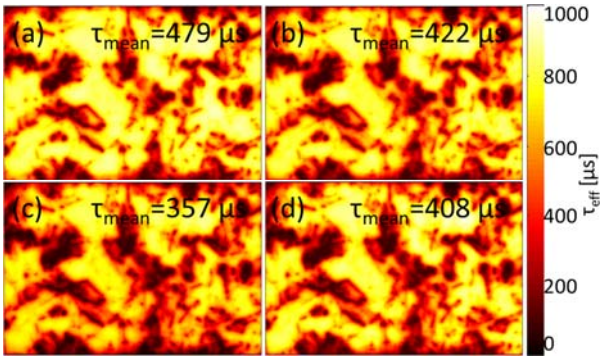

Figure 4 Lifetime calibrated PL images at an illumination intensity of 1 sun of the RTP sample (125 mm × 62.5 mm) "with plateau" at different time steps during degradation at ~1 sun and 75 °C. (a) Initial state, (b) after 16 hours of illumination, (c) after 105 hours, (d) after 339 hours. The scaling applies to all images.

significant degradation, the carrier lifetime staying at around 2.5 ms ($\Delta n = 10^{15}$ cm^{-3}). Therefore, we attribute the observed reduction of lifetimes exclusively to LeTID.

The only remaining differences between the samples in our study are the temperature profiles during the firing process, including slower ramp-up and ramp-down rates and a longer time above a given temperature in the case of the RTP-fired samples. One or a combination of these features consequently must have a significant influence on LeTID. The heterogeneous lifetime evolution of the FFO sample (Fig. 3) may be caused by a laterally inhomogeneous temperature profile which may be different at the edges. A similar effect was also noticed in [17].

4 Discussion It is well known that impurities and self-defects redistribute at elevated temperatures due to increased solubilities and diffusivities. Several mechanisms could explain the obviously favourable distribution resulting from RTP-typical temperature processes.

4.1 Internal gettering LeTID may originate from metallic impurities present in their dissolved, atomic state or as very small precipitates or atomic clusters that are activated e.g. by some complex formation during light exposure under elevated temperatures [11]. Since the distribution of metallic impurities is determined only by both the peak temperature and the cool down, with slower cooling rates facilitating the formation of large precipitates, it is conceivable that a slow cooling ramp decreases the share of LeTID precursors. In support of this hypothesis, the "denuded zone" observed around grain boundaries in the degraded state (Fig. 3) suggests that, in spite of the high firing rate and short time at elevated temperatures in the FFO process, the impurity atoms are internally gettered during the cool down (see also [17]). The theory is in line with previously published observations [9, 11, 12] that a high peak temperature is necessary to activate LeTID, promoting metallic precipitate dissolution, whereas a second fast firing step at a lower temperature reduces LeTID, which could support precipitate formation similar to a slow cool.

If a non-metallic impurity, such as oxygen, is part of the defect responsible for LeTID, the entire temperature history of the sample plays a role [18]. Nevertheless, the argumentation would run along the same lines.

4.2 Hydrogen diffusion It is plausible that hydrogen plays a role either by itself or in combination with an internal gettering effect discussed above. As stated in [19], the hydrogen content in the bulk increases with increasing peak temperatures of standard FFO processes (fast cool-down). If – at the same peak temperature – the peaking time is longer or a rather slow cool follows, then enhanced hydrogen effusion leads to a comparatively lower bulk hydrogen concentration. In this picture, hydrogen would form part of the LeTID complex: Higher peak temperatures in the FFO process lead to more hydrogen in the bulk and result in stronger LeTID [9, 11, 12]. Interestingly, the peak temperature "threshold" (FFO) for LeTID activation presented in [9] of around ~675 °C is very similar to the value of ~700 °C at which hydrogen release from the SiNx-layer is expected to start [19]. The lower cooling rate of the RTP processes would lead to a decreased H-concentration through enhanced H-effusion. A second firing step at moderate peak temperatures could have the same effect [9]. A further indication for the involvement of hydrogen comes from a study by Kersten et al. [20] who state that LeTID is suppressed if the (H-containing) dielectric layer is not present during the fast firing process. Please note that this conclusion stands in contrast with Nakayashiki's hypothesis that hydrogen passivates the LeTID complex [12].

To sum up, by manipulating the temperature profile of the firing process, light- and temperature-induced degradation in multicrystalline silicon can be significantly influenced. Samples fired with substantially lower ramp-up and cool-down rates virtually completely suppress LeTID even at very high peak firing temperatures. However, it is unclear whether the modification is specifically due to the change in ramp-up or ramp-down rates, or a combination of the two, resulting to changes in the thermal budget.

Supporting Information Additional supporting information may be found in the online version of this article at the publisher's website.

Acknowledgements The authors are indebted to Jonas Schön for very fruitful discussions. They acknowledge the financial support by the German Federal Ministry for Economic Affairs and Energy and by industry partners within the research cluster "SolarLIFE" (contract no. 0325763 A). The content is in the responsibility of the authors.

References

[1] M. A. Green, K. Emery, Y. Hishikawa, W. Warta, and E. D. Dunlop, Prog. Photovolt.: Res. Appl. **24**, 905–913 (2016), doi: 10.1002/pip.2788.
[2] K. Ramspeck, S. Zimmermann, H. Nagel, A. Metz, Y. Gassenbauer, B. Birkmann, and A. Seidl, in: Proc. 27th EU-PVSEC, Frankfurt, Germany, 2012, pp. 861–865.
[3] S. W. Glunz, S. Rein, J. Y. Lee, and W. Warta, J. Appl. Phys. **90**, 2397 (2001).
[4] J. Schmidt, K. Bothe, and R. Hezel, Appl. Phys. Lett. **80**, 4395–4397 (2002).
[5] D. H. Macdonald, J. Appl. Phys. **95**, 1021 (2004).
[6] F. Fertig, K. Krauß, and S. Rein, Phys. Status Solidi RRL **9**(1), 41–46 (2014).
[7] F. Kersten, P. Engelhart, H. C. Ploigt, A. Stekolnikov, T. Lindner, F. Stenzel, M. Bartzsch, A. Szpeth, K. Petter, J. Heitmann, and J. W. Mueller, Sol. Energy Mater. Sol. Cells **142**, 83–86 (2015).
[8] D. N. R. Payne, C. E. Chan, B. J. Hallam, B. Hoex, M. D. Abbott, S. R. Wenham, and D. M. Bagnall, Phys. Status Solidi RRL **10**(3), 237–241 (2016).
[9] C. E. Chan, D. N. R. Payne, B. J. Hallam, M. D. Abbott, T. H. Fung, A. M. Wenham, and S. R. Wenham, in: Proc. 43th IEEE-PVSC, Portland, USA, 2016.

[10] T. Luka, S. Eiternick, S. Frigge, C. Hagendorf, H. Mehlich, and M. Turek, in: Proc. 31st EU-PVSEC, Hamburg, 2015, Germany, pp. 826–828.
[11] D. Bredemeier, D. Walter, S. Herlufsen, and J. Schmidt, AIP Adv. **6**, 035119 (2016).
[12] K. Nakayashiki, J. Hofstetter, A. E. Morishige, T. A. Li, D. B. Needleman, M. A. Jensen, and T. Buonassisi, IEEE J. Photovoltaics **6**, 860–868 (2016).
[13] M. B. Shabani, T. Yamashita, and E. Morita, Solid State Phenom. **131–133**, 399–404 (2008).
[14] J. A. Giesecke, M. C. Schubert, B. Michl, F. Schindler, and W. Warta, Sol. Energy Mater. Sol. Cells **95**, 1011–1018 (2011).
[15] K. Bothe and J. Schmidt, J. Appl. Phys. **99**, 013701 (2006).
[16] L. J. Geerligs and D. Macdonald, Appl. Phys. Lett. **85**, 5227–5229 (2004).
[17] M. Selinger, W. Kwapil, F. Schindler, K. Krauß, F. Fertig, B. Michl, W. Warta, and M. C. Schubert, Energy Procedia **92**, 867–872 (2016).
[18] V. Voronkov and R. Falster, J. Cryst. Growth **204**(4), 462–474 (1990).
[19] S. Wilking, S. Ebert, A. Herguth, and G. Hahn, J. Appl. Phys. **114**, 194512 (2013).
[20] F. Kersten, J. Heitmann, and J. W. Müller, in: Proc. 32nd EU-PVSEC, Munich, 2016, Germany.